INTERNAL BEAM CURRENT INCREASE IN THE 680 MeV SYNCHRO-CYCLOTRON OF THE JOINT INSTITUTE FOR NUCLEAR RESEARCH

V. I. Danilov, I. B. Enchevich, B. I. Zamolodchikov,
B. N. Marchenko, D. L. Novikov, E. A. Polferov,
E. I. Rozanov, A. L. Savenkov, A. N. Safonov,
A. V. Shestov

Joint Institute of Nuclear Research (OIYaI), Dubna

(Presented by I. B. Enchevich)

Attempts have been made at the Laboratory for Nuclear Problems of the OIYaI to increase the intensity of the internal beam of the synchro-cyclotron. The work followed two directions: the establishment of an hf program of the synchro-cyclotron which would yield the maximum current at the final radius of the accelerator, and the creation of a focusing system which would compensate for the defocusing action of the space charge at the center of the accelerator [1] and thus increase the average current of the accelerated protons.

During the analysis of the phase motion within the synchro-cyclotron one can distinguish two basic steps: first is the capture of the particles at the center of the synchro-cyclotron into the accelerating cycle, and second is the phase motion during the acceleration up to the final radius.

To obtain the solution for the optimum capture of charged particles into the accelerating cycle within existing synchro-cyclotrons having an energy of several hundreds of millions of electron volts it does not suffice to analyze the phase equation of Bohm and Foldy [2]. This may be explained by the fact that the energy increment per turn during the first stage having a constant accelerating voltage (U_0 = const) depends on the radius of the orbit.

Figure 1 shows the curve of the relative proton energy increase per turn as a function of the radius. It is calculated for the potential field pattern of the dees on the model of the central region of the synchro-cyclotron of the OIYaI using an electrolytic tank. The quantity $\dot{\omega}_{s\ in}$, corresponding to the optimum trapping condition, we determined experimentally by measuring the current at the radius, R = 30 cm. The choice of this radius was dictated by the need to exclude the influence of changes in phase condition during the acceleration of protons in the region of medium and final radii. The quantity $\dot{\omega}_{s\ in}$ was changed over a wide range of varying magnetic field strengths at the center of the accelerator. For a voltage amplitude of U_0 = 12 kV on the dees and the existing geometry of the accelerating gap, the dependence of

$\dot{\omega}_{s\ in}$ for the OIYaI synchro-cyclotron is shown in Figure 2. The optimum magnitude of $\dot{\omega}_{s\ in}$ turned out to be $2.25 \cdot 10^{10}$ radians/sec^2 [3].

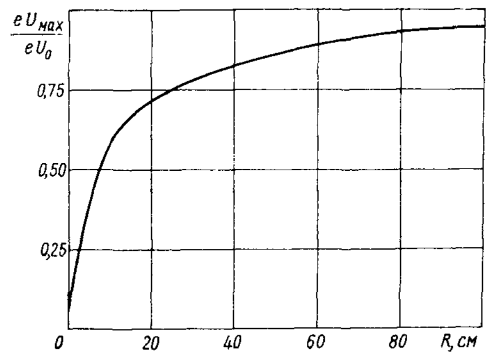

Figure 1. The relative energy increment as function of the radius of the orbit.

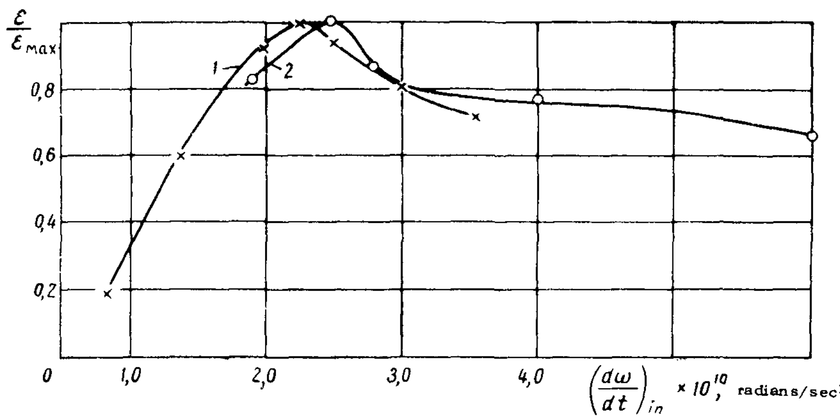

Figure 2. The dependence of the trapping efficiency on the derivative dω/df at the start of acceleration:

1 -- Prior to the changes in the resonant system; 2 -- after the changes.

By correcting the parameters of the resonant system of the accelerator in January of 1961, we achieved a frequency program having the desired value of $\dot{\omega}_s$ at the start of the acceleration (Figure 3, curve 2) which resulted in an internal beam current increase from 0.3 to 0.8 μA at the final radius R = 274.5 cm. The proton current was measured by the activity induced in an aluminum target (reaction $Al^{27}(p, 3pn)Na^{24}$) irradiated at the R = 270--280 cm radii. The target, having a lead base, was calibrated on the external synchro-cyclotron proton beam utilizing a Faraday cylinder.

The second round consists of the construction of such an hf characteristic of the synchro-cyclotron $\omega_s = \omega_s(t)$ and $U_0 = U_0(\omega_s)$, which would simultaneously guarantee the optimum trapping condition for the ions and their subsequent acceleration up to the final radius without phase losses.

During the selection of the frequency program for the synchro-cyclotron we took into account the damping of phase oscillations in the proton acceleration process up to the final accelerator radius; we utilized the invariance of the action integral J during an adiabatic change in the parameters of the system. In the given case

$$J = \oint I\dot{\varphi}\, d\varphi, \quad I = \frac{E_s}{\omega_s^2 K_s}, \quad K_s = 1 + \frac{n}{1-n}\cdot\frac{1}{\beta_s^2},$$

$$\dot{\varphi} = \sqrt{\frac{2eU_0\omega_s^2 K_s}{\pi\varepsilon_s}}\sqrt{\cos\varphi_s + \varphi\sin\varphi_s + g},$$

where g is an integration constant.

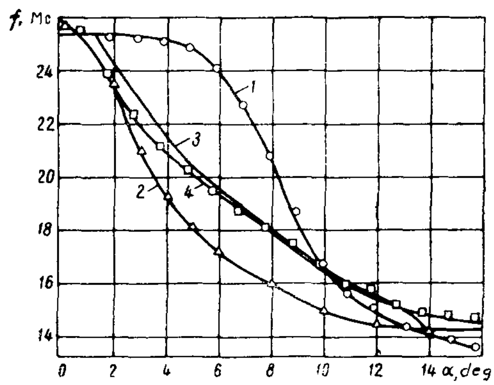

Figure 3. Frequency characteristics of the resonant system of the synchro-cyclotron (α is the angle of rotation of the buncher).

For the limit of the region of phase stability the dependence of $\varphi = \oint \dot{\varphi}\, d\varphi$ on $\sin\varphi_s$ was obtained by numerical integration. Using the $\psi = \psi(\sin\varphi_s)$ dependence, one can determine the permissible increase in $\sin\varphi_s$ for which all the accelerated particles found within the region of stationary phase oscillations in the $(\varphi, \dot{\varphi})$ plane at the beginning of the acceleration will not leave this region during the acceleration process, and from the relationships found, $\sin\varphi_s = f(R)$, one can calculate the corresponding frequency-time characteristics $\omega_s = \omega_s(t)$. Such a characteristic is shown in Figure 3 (curve 3). The same figure shows the frequency characteristic (curve 4) which was obtained at the end of 1961 after supplying the buncher with stator blocks of new shape. As can be seen from the figure, the experimental characteristic is close to the calculated one. Curve 1 corresponds to the state of affairs existing prior to 1961. The shape of the experimentally determined new blocks is shown in Figure 4. Figure 5 compares the current changes along the radius for two hf characteristics. It is clear from the comparison of these curves that we basically removed the phase losses within the R = 30--80 cm range of radii. This led to the increase of proton current up to 1.1--1.2 μA at the final radius.

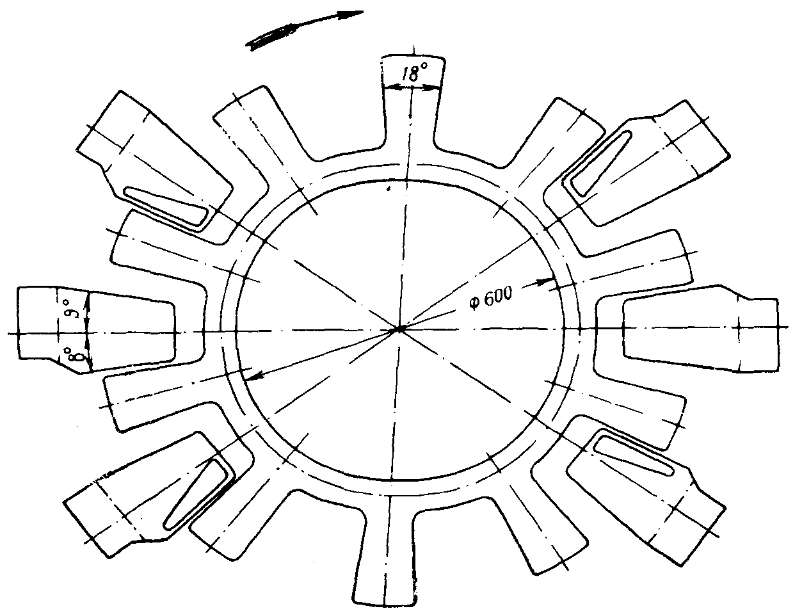

Figure 4. The location of the new blocks within the buncher.

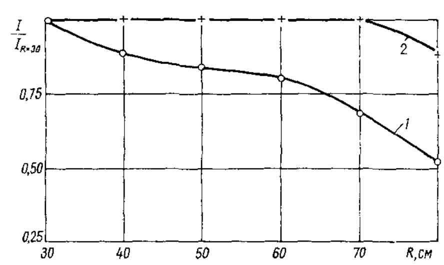

Figure 5. Relative current decrease along the radius:

1 -- With phase losses; 2 -- without phase losses.

A further increase in synchro-cyclotron intensity was achieved by the introduction of additional vertical (axial) focusing of the beam within the central region of the accelerator. Studies of the focusing system showed the advantage of electrostatic as compared with the magnetic focusing at the center of the accelerator. These advantages are due to the relatively low values of the constant electrode potential (the ion energy is still small), the simplicity of construction of such a system under the condition of increased radiation, and the possibility of a wide range of control in its focusing characteristics.

The system of electrodes used within the OIYaI synchrocyclotron is shown in Figure 6. The design provides for possible variation in the gap between the dee and the auxiliary electrodes. In addition, the configuration of the electric field can be changed by varying the position of the grounded screens located between the dee and the potential electrodes. The potential electrodes are capacitatively locked in with the hf guides of the basic dee.

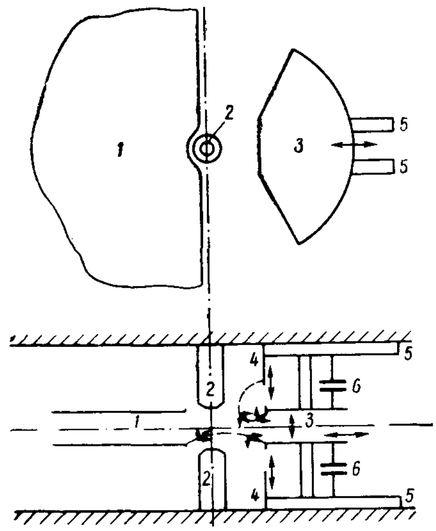

Figure 6. The distribution of focusing electrodes within the accelerator chamber:

1 -- The basic dee; 2 -- ion source; 3 -- focusing electrodes; 4 -- screens; 5 -- controls; 6 -- capacitors.

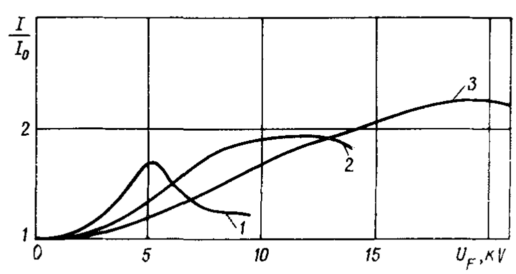

Figure 7. Current increase as a function of the focusing voltage U_F (electrode distance from the center is 0.1 (1), 0.15 (2), and 0.2 (3), respectively).

The ion motion within the magnetic field of the accelerator and the auxiliary electrostatic field formed by the added electrodes can be described by the Hill equation. The additional vertical forces are fixed by the shape of the electric field found on the model of the central part of the accelerator chamber using an electrolytic tank. The necessary electric field component E_z for the production of additional vertical focusing forces was found, as function of the azimuth, orbit radius, and its distance from the median plane, by differentiating the measured potential with respect to z.

Experimental studies of the properties of the above-mentioned system yielded the optimum location of the focusing device electrodes based on the beam current dependence on U_F for various electrode distances from the center of the accelerator (Figure 7). Using these results and taking into consideration the reliability of operation we chose the following parameters:

The distance of the front edge of the electrodes from the center................	150 mm
Gap between the electrodes and the screen....	-30 mm
Focusing voltage U_F.........................	-13 kV

The internal beam current under these conditions increased approximately by a factor of two and at the present time is 2.2--2.3 μA.

BIBLIOGRAPHY

1. Keller, R., Fidecaro, M., Barbier, M. CERN 57-45 (1957).
2. Bohm. D., Foldy, L. Phys. Rev., Vol 72, 649 (1947).
3. Zamolodchikov, B. I., Novikov, D. L., Polferov, E. A. Preprint OIYaI R-720, Dubna, 1961.